Citation: Molecular Therapy—Nucleic Acids (2016) 5, e315; doi:10.1038/mtna.2016.27
Official journal of the American Society of Gene & Cell Therapy
www.nature.com/mtna

In Vivo Selection Against Human Colorectal Cancer Xenografts Identifies an Aptamer That Targets RNA Helicase Protein DHX9

Jing Mi[1], Partha Ray[1], Jenny Liu[1], Chien-Tsun Kuan[2], Jennifer Xu[1], David Hsu[3], Bruce A Sullenger[1], Rebekah R White[1] and Bryan M Clary[4]

The ability to selectively target disease-related tissues with molecules is critical to the design of effective therapeutic and diagnostic reagents. Recognizing the differences between the *in vivo* environment and *in vitro* conditions, we employed an *in vivo* selection strategy to identify RNA aptamers (targeting motifs) that could localize to tumor *in situ*. One of the selected molecules is an aptamer that binds to the protein DHX9, an RNA helicase that is known to be upregulated in colorectal cancer. Upon systemic administration, the aptamer preferentially localized to the nucleus of cancer cells *in vivo* and thus has the potential to be used for targeted delivery.

Molecular Therapy—Nucleic Acids (2016) **5**, e315; doi:10.1038/mtna.2016.27; published online 26 April 2016
Subject Category: Aptamers

Introduction

Colorectal cancer is one of the leading causes of cancer-related mortality in the United States and is usually incurable if distant metastases are present.[1] Defining the differences between cancer and normal tissues will facilitate the development of agents to specifically target cancer. These targeted agents may themselves be capable of inhibiting the growth or invasion of cancer cells, or they may allow the delivery of non-specific toxic cargo specifically to cancer cells. Specificity for cancer cells is necessary to minimize toxicity to normal tissues.

Aptamers are a class of artificial oligonucleotides with the ability to fold into precise three-dimensional and globular confirmations that enable them to directly and specifically bind to targeted proteins, and are thus ideal for targeted molecular therapy.[2–4] The Systematic Evolution of Ligands by Exponential Enrichment (SELEX) method is typically applied to select aptamers *in vitro* against purified protein, complex-protein mixtures or whole cells.[5–7] However, one of the drawbacks of *in vitro* SELEX generated aptamers is that often an *in vitro*-selected aptamer fails to bind to the protein target *in vivo* and thus is ineffective in animal models. One possible reason for this difference might be that aptamer binding is dependent on its protein target conformation, which is in turn affected by the target's environment and can vary between the *in vitro* and *in vivo* setting.

In our previous work, we developed a novel *in vivo* SELEX strategy where, instead of using an *in vitro* cell culture system or purified proteins, the whole experimental animal was used for aptamer generation.[2] With this type of selection technique, it is feasible to develop aptamers that could selectively recognize diseased organs or tissues within the test subjects. Since properties like bioavailability, systemic circulation time, and tissue distribution of the aptamers are embedded in the *in vivo* selection scheme itself, this scheme potentially decreases the pharmacologic optimization that would otherwise need to be performed postselection. Using this novel selection strategy, we screened a large library of nuclease-resistant RNA oligonucleotides in mice bearing murine CT26 colon carcinoma liver metastases to identify RNA aptamers that can localize to intrahepatic tumor deposits. One of the selected aptamers targeted p68, an RNA helicase that has been shown to be upregulated in colorectal cancer.

In our present work, we have further refined the *in vivo* selection strategy with the intention to create a more clinically relevant reagent that can be extended in human patients. To accomplish this goal, we established intrahepatic xenografts in immunodeficient mice using two cell lines (designated 119X and 57X) derived from human patients undergoing liver resection for colorectal liver metastases (Pro00002435). Two separate *in vivo* selections were performed using xenografts derived only from the 119X or 57X cell lines, with the aim to identify cell line-specific aptamers. A third selection scheme, that comprised of toggling the aptamer selection process[8] between xenografts derived from the 119X and 57X cell lines, was performed with the intention to identify aptamers that would recognize targets that might be present on both xenografts.

Results

In vivo selection of RNA aptamers that localize to human colon carcinoma

In vivo selection of RNA was performed on an animal model of hepatic colorectal cancer metastases whereby nude mice bearing a previously implanted human xenograft were

The first two authors contributed equally to this work.
[1]Department of Surgery, Duke University Medical Center, Durham, North Carolina, USA; [2]Department of Pathology, Duke University Medical Center, Durham, North Carolina, USA; [3]Department of Medicine, Duke University Medical Center, Durham, North Carolina, USA; [4]Department of Surgery, University of California at San Diego, La Jolla, California, USA. Correspondence: Bryan M Clary, Department of Surgery, University of California at San Diego, La Jolla, California 92093, USA. E-mail: bclary@ucsd.edu Jing Mi, Department of Surgery, Duke University Medical Center, Durham, NC 27710. E-mail: jing.mi@duke.edu
Keywords: aptamer; colorectal cancer; *in vivo* SELEX
Received 19 October 2015; accepted 10 March 2016; published online 26 April 2016. doi:10.1038/mtna.2016.27

inoculated with a randomized library of 2′fluoropyrimidine-modified RNA library sequences. In an effort to negatively select against sequences that nonspecifically distribute to a variety of tissues, the library was injected systemically and allowed to circulate prior to purging the circulation and harvesting the tumor. To monitor for the enrichment of RNA aptamers in the selected pool at various rounds, the *in vitro* binding affinity against tumor extracted protein was assessed. During successive rounds of selection, RNA pools demonstrated increased binding for tumor protein extract as compared with the control RNA library (**Figure 1a**). After 12 rounds of *in vivo* selection, the enriched RNA pool was cloned and sequenced. Sequences were analyzed and sorted into families by alignment. Interestingly, two predominant RNA families, represented as Family A and Family B, were obtained. Both families, each represented by a dominant sequence, were present in all three selection schemes but with different percentages of representation (**Figure 1b**). Notably, the sequences from Family A and Family B differed considerably, indicating the possibility of different protein targets. In theory, the identification of identical sequences in three independent selections with an N40 library is astronomically low. We reason that when the starting DNA template was transcribed, specific sequences may have been represented multiple times in the starting RNA library, which was then divided for the separate selections. Therefore, while the presence of the same sequences in independent selections may indicate a bias toward the sequences based on transcription or amplification efficiency, it is not necessarily the result of cross-contamination. One specific RNA molecule, S-1 from Family A, had a slightly higher representation in the three selection schemes and was chosen for further characterization.

First, we confirmed the binding affinity of S1 aptamer against tumor protein extracts. In comparison to the starting library, S-1 displayed threefold higher binding affinity for tumor protein extract in ^{32}P-based filter binding assay (**Figure 1c**). Additionally, S-1 displayed much lower binding affinity when it was tested against normal colon or normal liver protein extracts, indicating that it selectively recognizes a target that is more abundant in colon carcinoma (**Figure 1d**,**e**).

Next, we investigated whether the selected aptamer S-1 is capable of specifically localizing to tumors *in vivo*. For this, tumor-bearing mice were administered intravenous injections of Cy3-labeled RNAs and a tumor marker MMPSense 750, then subjected to fluorescence molecular tomography (FMT) imaging (**Figure 2a**,**b**). S-1 RNA signal was found to localize to 119X xenograft with fivefold specificity over library RNAs (**Figure 2a**). Approximately 95 pmol (5% of injected dose) was retained in the implanted tumors after 1.5 hours. Also, S-1 RNA's tumor localization was observed as early as 10 minutes postinjection, when no significant tumor localization was observed in the RNA library control (**Figure 2b**). There was minimal fluorescence in adjacent normal liver tissue based on the figure. Additionally, *ex vivo* comparison was performed to validate the *in vivo* imaging data. After FMT *in vivo* imaging, tumor-bearing liver tissues were excised and imaged again. The fluorescence intensity profile in all groups (**Figure 2c**) is highly consistent with their corresponding 2D images, which indicates the feasibility and sensitivity of FMT for the detection and quantification of tumor-targeting aptamer in the liver metastasis model. Together, these data indicate that selected S-1 aptamer has promising tumor trafficking ability and could be used for escorting therapeutic cargo to tumors *in vivo*.

Identification of the protein target of the aptamer S-1

In order to identify the binding partner of the selected aptamer S1, an affinity purification protocol was applied as described previously.[2] The biotinylated S1 aptamer-bound protein was eluted in the denaturing biotin elution buffer. Upon resolving the eluted protein on a sodium dodecyl sulfate-polyacrylamide gel electrophoresis gel, it was stained with Coomassie Blue. A polypeptide band migrating around ~150 kDa was detected. No detectable bands were visualized when the same technique was performed using the control RNA library, thus indicating the specificity of the affinity purification protocol (**Figure 3a**). Next, the Coomassie-stained band was subjected to peptide mass finger-printing method to identify the protein. Human ATP-dependent RNA helicase A (DHX9) was identified through this process. DHX9 is known to function as a transcriptional regulator and has been implicated in cellular proliferation and/or neoplastic transformation.[9–11] In order to further verify the target identification, Western blot and immunohistochemistry (IHC) analyses were performed. The data from the Western blot assay demonstrated that the protein DHX9 was found to be highly expressed in both tumor cell lines (57X and 119X) and their xenotransplanted tumor tissues. Notably, no detectable staining was observed in extracts from normal colon epithelial cells (CCD-18Co) nor in the liver and colon extracts harvested from normal wild-type mice. Similarly, in the IHC analysis of 119X xenograft tissue, DHX9 antibody stained only in the region of tumor but not adjacent normal tissues, as delineated by H&E staining (**Figure 1b**,**c**).

To characterize the affinity of aptamer S-1 binding for protein DHX9 *in vitro*, first we utilized surface plasmon resonance (SPR) analysis using protein DHX9 immobilized on a Biacore chip. Compared with the unselected library RNA, S-1 has a much higher association rate (7.2e6 versus 1.7e5 library) and lower dissociation rate (1.4e–7 versus 6e–6 library) at the concentration of 500 nmol/l (**Figure 4a** left and middle). This binding affinity is comparable to DHX9 antibody (data not shown). As a negative protein control, bovine serum albumin (BSA) was used in SPR measurement, and there was no meaningful binding with S-1 (**Figure 4a** right) as indicated by the very low R_{max}. Also, in another SPR experiment using nucleophosmin, another RNA binding protein, to determine the binding specificity of S-1 with DHX9, there was no significant binding (data not shown). These data indicate that S-1 binds DHX9 with very high affinity and specificity, a characteristic that is ideal for drug delivery or imaging purposes.

Next, we wanted to ascertain whether selected aptamer S-1 colocalizes with DHX9 in the tumor region. To this end, cryostat tumor sections were prepared after intravenous injection of Cy3-labeled RNAs and a perfusion marker, Hoechst, into tumor bearing mice. Due to the poor vascularization in the tumor, Hoechst does not stain the tumor and it is visualized as a dark region. *In vitro* immunostaining with DHX9 antibody was then performed (**Figure 4b**). Tumor tissue sections stained with DHX9 antibody displayed overexpression

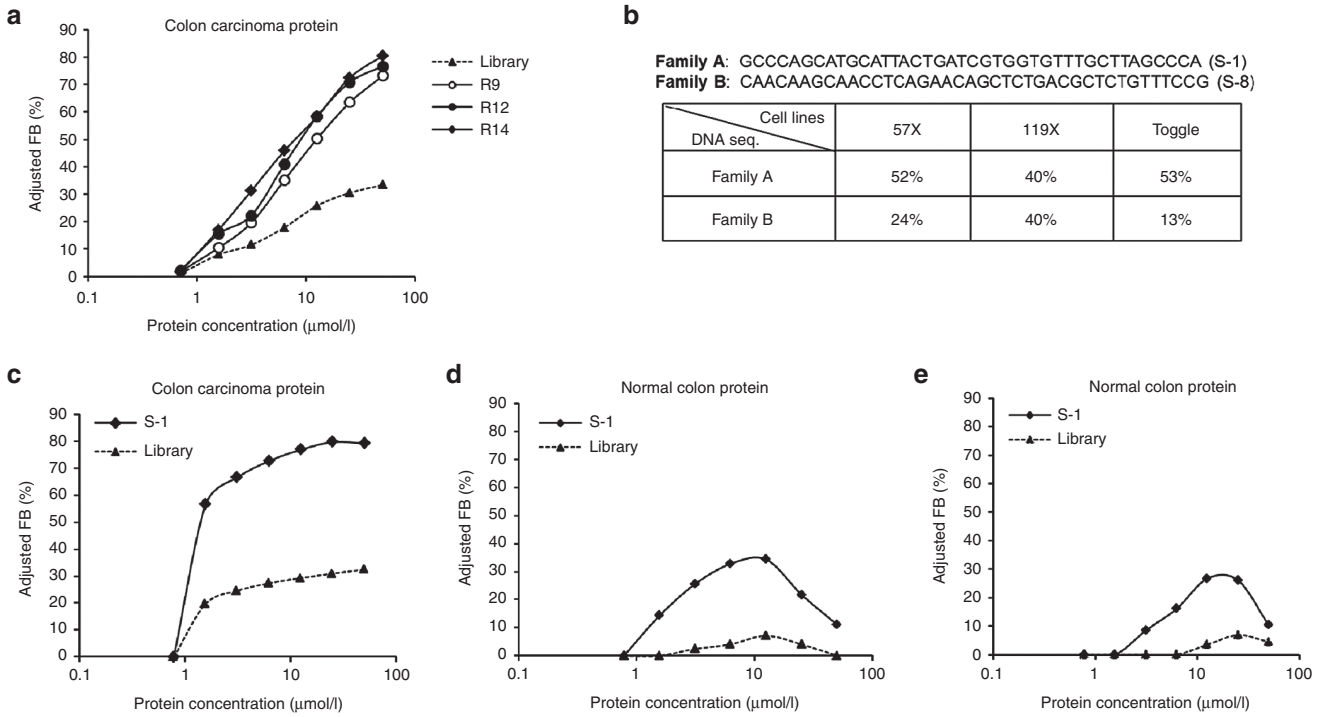

Figure 1 Intrahepatic tumor-evolved *in vivo* RNA selection pools. RNA pools from rounds 14, 12, 9 and the starting round were assayed for binding to tumor protein extract (**a**). RNA pool of round 12 was sequenced and their random region sequences as well as their representation in each *in vivo* selection are shown in the table (**b**). RNA S-1 was assayed for binding to tumor protein extract (**c**) and control protein extracted from normal colon (**d**) and liver tissue (**e**).

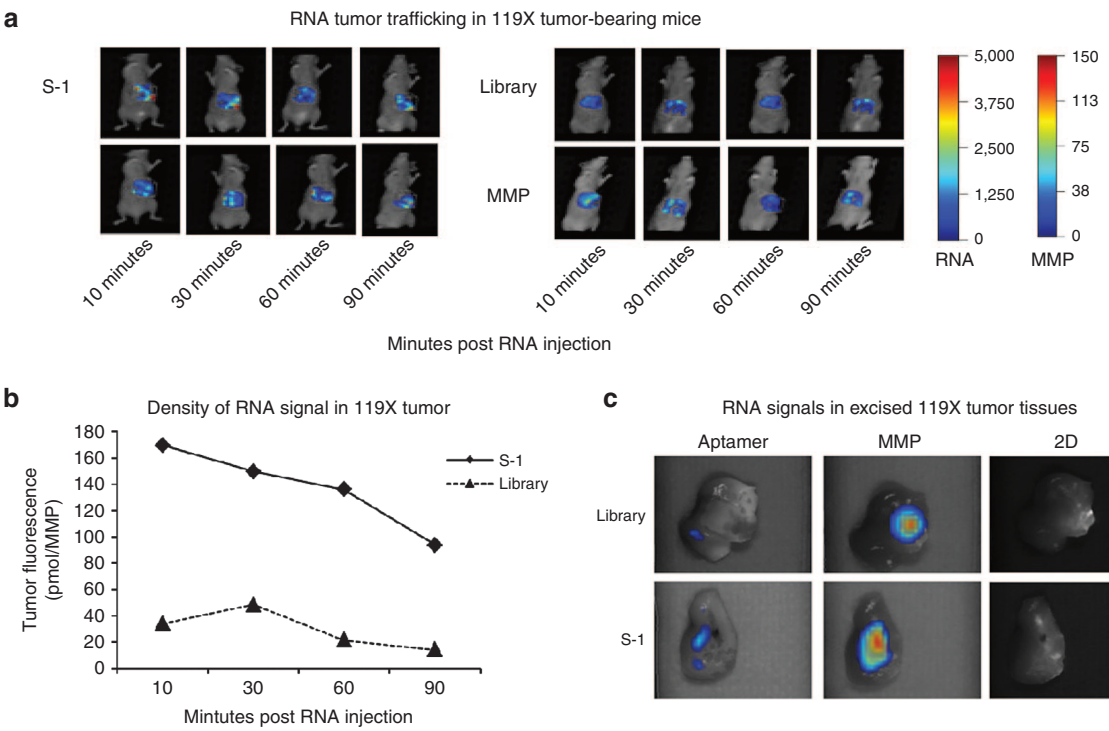

Figure 2 *In vivo* FMT imaging and quantification of RNA signal in intrahepatic colon cancer-bearing mice. FMT images of representative 119X xenotransplants (**a**). The total amount of fluorescence (pmol) was quantified in specific ROIs encompassing each tumor. Due to the difference of tumor size in each animal, the signal density was normalized by the signal of tumor marker MMPsense 750 at various times (**b**). *Ex vivo* validation of fluorescence signals in excised 119X tumor tissues coinjected with RNA and tumor marker MMPsense 750 (**c**). FMT, fluorescence molecular tomography.

of DHX9 when compared with corresponding normal tissues, consistent with the IHC result (**Figure 3c**). In mice treated with Cy3-labeled S-1, red fluorescence was exclusively restricted to the tumor area, a region that is characterized by poor perfusion of Hoechst in blue (**Figure 4b**). This finding is also consistent with our FMT imaging data (**Figure 2**). By contrast, red fluorescence was not detected in Cy3-labeled RNA library-treated animal. When double staining with anti-DHX9 antibody (fluorescein isothiocyanate, green) and aptamer S-1 (Cy3, red) was performed, the stained regions overlapped. This indicates that the epitope recognized by the antibody is different than the aptamer-binding region on DHX9 protein.

In order to help confirm that S-1 is specifically binding to DHX9, we knocked down DHX9 protein expression in the 119X cell line using RNA interference. Western blot analysis indicated a twofold reduction in DHX9 protein level in cells transfected with DHX9 small interfering RNA (siRNA) as compared cells transfected with control siRNA (**Figure 5a**). The cell-free extract from DHX9 siRNA-treated cells was then subjected to ^{32}P-labeled S-1 aptamer radioactive filter binding assay. S-1 binding to the DHX9 siRNA-treated cell extract was substantially reduced as compared with the control siRNA-treated cells (**Figure 5b**). The concomitant reduction in DHX9 protein level with reduction in S-1 binding to the cell extract strongly support that DHX9 is the protein binding partner of S-1 aptamer (**Figure 5a**).

Finally, the subcellular localization of aptamers was investigated using fluorescence microscopy. Cy3-labeled aptamer S-1 stained nonpermeabilized 119X cells much more intensely than Cy3-labeled RNA library (**Figure 6a**). Counterstaining the cellular nuclei with 4,6-diamidino-2-phenylindole and the cytoplasm with AlexaFluor 488-labeled actin probe phalloidin revealed that aptamer S-1 is localized in the nucleus as well as the cytoplasm. We then triple-stained permeabilized tumor cells with aptamer, 4,6-diamidino-2-phenylindole, and anti-DHX9 antibody to replace phalloidin to examine the colocalization of the aptamer and antibody (**Figure 6b**). The resulting staining pattern of aptamer S-1 was consistent with that of anti-DHX9 antibody. The staining was mainly localized in the nucleus with only a small amount found in the cytoplasm. With the control RNA library, a slight background staining was observed in the cytoplasm. The labelling pattern of aptamer S-1 differed between **Figure 6a** (cytoplasmic and nuclear) as compared with **Figure 6b** (predominantly nuclear). This is probably due to the necessity of permeabilizing the cells before costaining them with the DHX9 antibody, allowing the aptamer to migrate freely to the cell nucleus. The data in **Figure 6a**, however, indicate that aptamer S-1 can actively enter living cells and bind the target protein, which is predominantly localized in the nucleus.

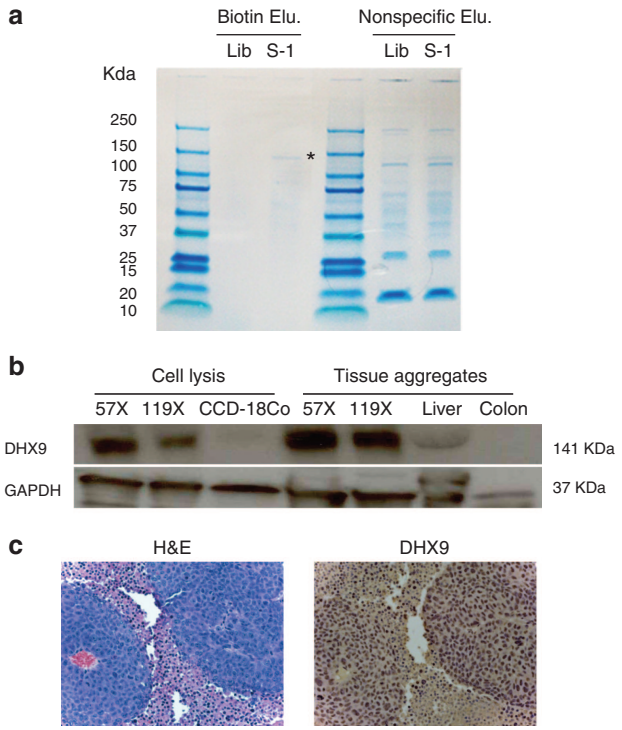

Figure 3 Identification of tumor-specific protein. Commassie blue-stained SDS-PAGE gel analyzing the aptamer S-1-mediated target protein purification. Lanes 1 and 4, molecular marker; lanes 2 and 5, purification with control aptamer library as a probe control; lanes 3 and 6, purification with aptamer S-1; lanes 2 and 3, RNA-binding protein complexes eluted by biotin elution buffer; lanes 5 and 6, RNA-binding protein complex eluted by nonspecific Laemmli sample buffer as an elution buffer control (**a**). Western blot analyses of the expression of aptamer S-1 in both tumor cell lines and tissues by anti-DHX9 antibody. The sample loading amounts were normalized based on their protein concentration and GAPDH expression (**b**). Immunohistochemical staining of DHX9 in tumors excised from 119X intrahepatic tumor nodules (**c**). Tumor area is depicted by H&E stains (left) and DHX9 expression by anti-DHX9 antibody (right). SDS-PAGE, sodium dodecyl sulfate-polyacrylamide gel electrophoresis gel.

Discussion

We designed an *in vivo* selection strategy to identify RNA aptamers capable of localizing to a target, in this case a tumor, in a biological system under physiological conditions. This *in vivo* selection strategy differs from conventional *in vitro* SELEX approaches in a few ways. First, traditional SELEX directly selects for aptamers on the basis of high-affinity binding to a specific target protein. Such ligands may or may not localize to targets *in vivo*. *In vivo* selection, in contrast, is performed without directly selecting for binding to a specific target protein but rather by selecting for localization to a specific tissue. Second, because of structural differences in protein conformation, aptamers generated by *in vitro* SELEX that bind a protein in its purified form may not bind the same target in its natural environment, a problem avoided with *in vivo* selection. Third, *in vivo* selection takes advantage of a "built in" negative selection, in which RNA aptamers that disperse to normal organs/tissues are selected out with successive rounds.

We previously demonstrated proof-of-concept that *in vivo* SELEX can be used to generate aptamers that localize to murine tumors. In order to generate a reagent that could be translated to human patients, we repeated a similar selection strategy using xenografts derived from human patients with metastatic colon cancer. The selected aptamer (S-1) preferentially binds to tumor over normal tissue extracts, suggesting that the aptamer recognizes a target that is overexpressed

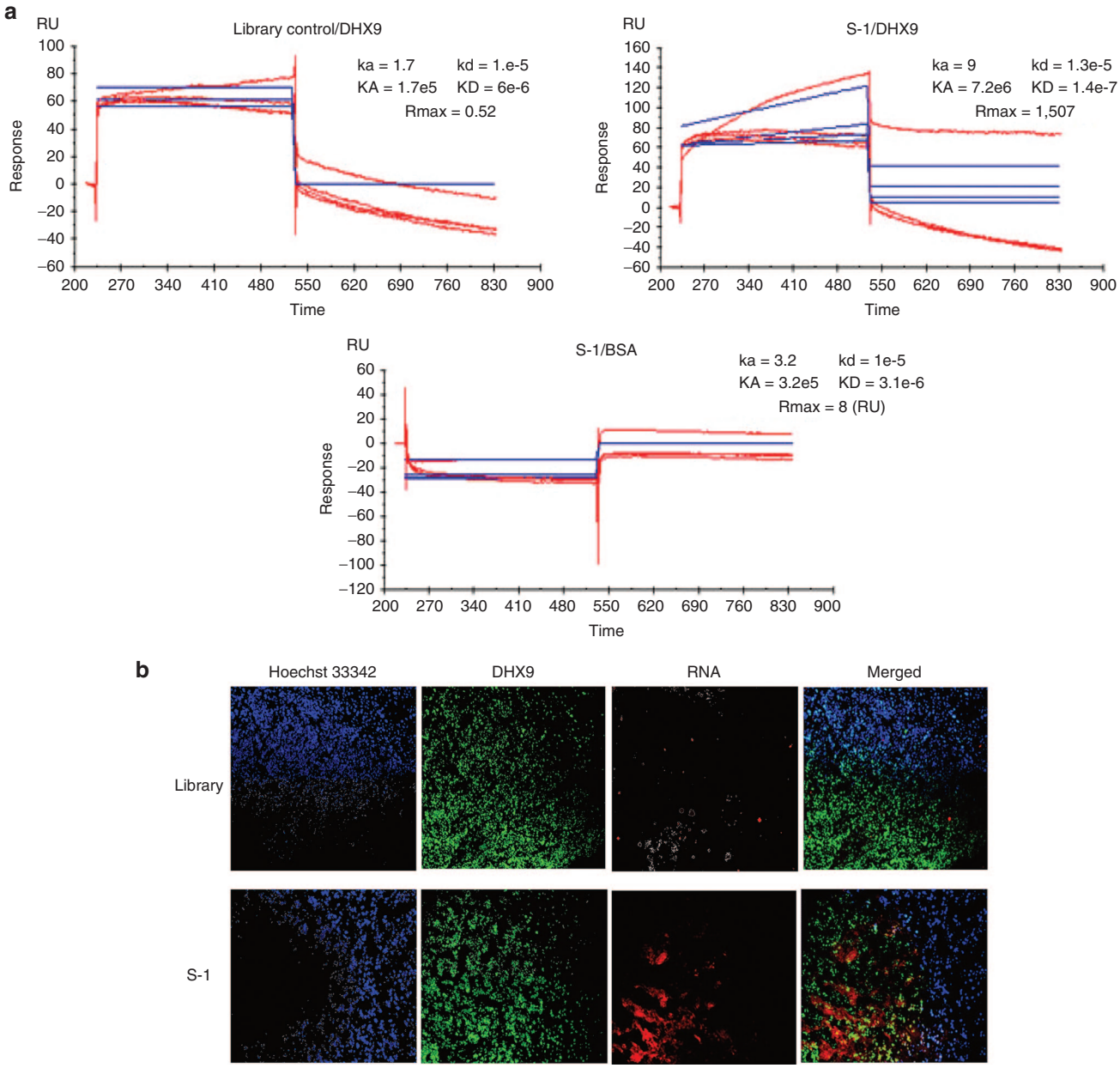

Figure 4 The binding of aptamer S-1 with its target protein. The interaction between protein DHX9 and aptamer S-1 is confirmed by SPR at the protein concentrations ranging from 62.5 to 500 nmol/l. Also, library and BSA were used as aptamer S-1 and protein DHX9 negative control, respectively (**a**). Representative fluorescence microscopy reveals the distribution of RNA molecules[23] in tumor, the region that is characterized by poor perfusion of Hoechst 33342 (blue) after intravenous injection. The majority of aptamer S-1 was colocalized with DHX9 expression tumor (green) and not adjacent normal liver tissue (lower panel). Control library RNA did not colocalize with DHX9 (upper panel) (**b**). SPR, surface plasmon resonance.

on colorectal cancer cells as compared with normal tissue. Affinity purification and peptide-mass fingerprinting identified S-1's binding partner as protein DHX9, also known as RNA helicase A or Nuclear DNA Helicase II. The SPR analyses with purified DHX9 protein provide confirmation that RNA S-1 is an aptamer that binds to DHX9 with high affinity and specificity.

DHX9 protein is involved in transcriptional and translational regulation, DNA replication/repair, and maintenance of genome stability. DHX9 is expressed in all cells, and knockdown of DHX9 in primary human fibroblasts causes premature senescence (irreversible growth arrest).[12] DHX9 is a monomeric protein of molecular weight ~140 kDa and contains a helicase domain that unwinds double-stranded DNA and RNA in a nucleotide-dependent manner. The catalytic helicase domain is flanked by two double-stranded RNA binding domains at the N-terminus and an arginine–glycine-rich region (RGG domain) at the C-terminus. A bidirectional nuclear transport domain is also present at the C-terminus. DHX9 has been shown to shuttle between the nucleus and

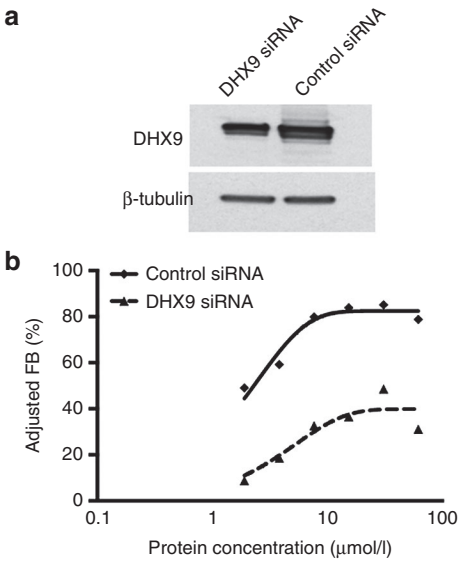

Figure 5 Knockdown of DHX9 protein. Western blot analysis of DHX9 protein in DHX9 siRNA and control siRNA-transfected cell extracts; protein loading was normalized to β-tubulin (**a**). Aptamer S-1 was assayed for binding to protein extract form DHX9 siRNA-transfected cells and compared with the control siRNA-transfected cell extract (**b**).

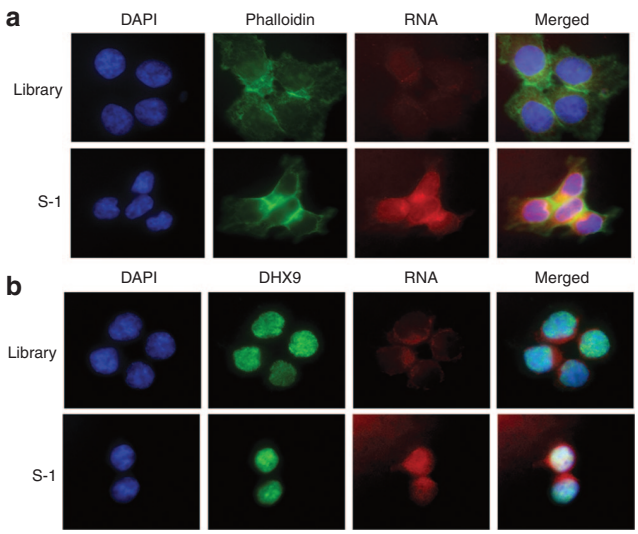

Figure 6 Aptamer S-1 internalizes into human colon carcinoma cells. Fixed 119X cells were stained using Cy3-labeled aptamer S-1[23], cytoskeleton probe AlexaFluor 488 phalloidin (green) and nuclear staining dye DAPI (blue). Merged, colocalized areas appear pink (red/blue) for nuclear-localized aptamer and light green (red/green) for cytoplasm-localized aptamer (**a**). Fixed 119X cells were stained by Cy3-labeled aptamer,[23] FITC-labeled anti-DHX9 antibody (green) and DAPI (blue). Merged, colocalized areas appear light blue (blue/green) for nuclear-localized DHX9 and bright white (blue/green/red) for colocalization of S-1 and DHX9 (**b**). DAPI, 4,6-diamidino-2-phenylindole.

the cytoplasm.[13,14] We demonstrated that Cy3-labeled S1 aptamer labeled both the nucleus and cytoplasm of tumor cells by fluorescence microscopy, corroborating this finding. Our previous *in vivo* selection yielded an aptamer that targets another helicase, p68, which shuttles between the nucleus and cytoplasm as well and has been shown to be present on the cell surface of HeLa cells by other group.[15] Moreover, nucleolin, another RNA helicase involved in ribosome biogenesis, has been shown to function as a cell surface receptor and act as a shuttling protein to help coordinate extracellular and nuclear events.[16] Based on the above observations, we speculate that aptamer S-1 is taken up into cancer cells by binding to DHX9 protein that is known to shuttle to the cytoplasm and—similar to nucleolin and p68—may also be transiently shuttling to the cell surface in cancer cells.

In addition to its established ATP-dependent RNA helicase activities,[17] DHX9 is overexpressed in various types of cancers[18] and has important interactions with IGF2 in pediatric cancers,[9] BRCA1 and BAP1 in breast cancer,[19] and SOX4 in prostate cancer.[10] DHX9 also maps to chromosome 1q25 near a major susceptibility locus for prostate cancer.[20] However, a relationship of DHX9 with colon cancer has not previously been reported.

We found that DHX9 is overexpressed in colorectal cancer cell lines derived from two different patients as well as the corresponding xenograft tumor tissue. The S-1 aptamer binds to DHX9 and localizes to tumors *in vivo*. We envision that reagents, which target nucleic acid binding proteins that shuttle to and from the nucleus, may facilitate targeted delivery to the nucleus. Further studies will be conducted to test whether S-1 may serve as a tool to escort therapeutic cargo specifically into tumor cells.

Materials and methods

Intrahepatic tumor model. Six- to eight-week-old female immunodeficient mice (nu/nu, Duke Cancer Center Isolation Facility) were anesthetized with 2% vaporized isoflurane and administered an intrahepatic injection of 10^6 57X or 119X human colon carcinoma cells. Postinjection bleeding and tumor cell leakage were avoided by brief local compression. A single tumor nodule in each mouse was allowed to grow for 20 days. All animal procedures were performed according to the standards of the Institutional Animal Care and Use Committee.

DNA library design and in vitro RNA production. A synthetic DNA pool (QIAGEN, Valencia, CA) of sequence 5′-GGGGGA ATTCTAATACGACTCACTATAGGGAGGACGATGCGG(N40) CAGACGACTCGCTGAGGATCCGAGA-3′, where N40 represents 40 random nucleotides, was amplified by PCR with primers (forward primer 5′-GGGGGAATTCTAATACGACTC ACTATAGGGAGGACGATGCGG-3′ and reverse primer 5′-TCTCGGATCCTCAGCGAGTCGTC-3′), and a T7 promoter sequence was incorporated into 5′ primers as previously described.[2] The reaction was accomplished with 20 amplification cycles using the following cycling parameters: 30 seconds at 95 °C, 30 seconds at 55 °C, and 30 seconds at 72 °C. The expected product size was 107 bp. The PCR product was then transcribed *in vitro* using a DuraScribeTM T7 Transcription Kit (Epicentre, Madison, WI), where 2′-Fluro (2′-F) pyrimidines were incorporated to produce modified RNA to protect against nucleases and, therefore, were

amenable to *in vivo* utility. The reaction was accomplished by incubation at 42 °C for overnight and subsequent purification by chromatography. The expected aptamer size was 80 bp.

In vivo selection procedure. In vivo selection was performed on tumor-bearing mice using a similar protocol as described previously.[2] Briefly, 5 nmol of RNA aptamer pool in 200-µl PBS was injected into the tail vein of mice. Mice injected with PBS were used as a control. Considering that aptamers can escape the vasculature within 10 minutes after injection, and that the liver is a predominant organ to which the aptamer would be distributed, we chose to kill the mice between 20 and 30 minutes after injection. The mice were killed by heart perfusion to remove blood from the liver, and total RNA was extracted from tumor tissue and reverse transcribed with the reverse primer. The bound cDNA was PCR amplified, and aptamer was then generated by *in vitro* transcription following the same procedure as described earlier.[2] The resulting pool containing reduced complexity RNA oligonucleotides was used for the next round of selection. To monitor aptamer pool enrichment at various rounds, the pool's affinity against tumor proteins was determined using the binding assay described below.

Tissue protein extraction and aptamer binding assay. For binding assays and later target protein purification work, tissue proteins were extracted from intrahepatic tumors with a T-PER Tissue Protein Extraction kit (Pierce, Rockford, IL). Briefly, 1 g of tissue was homogenized in 20 ml of T-PER reagent containing protease inhibitors (Roche Diagnostics, Mannheim, Germany) for 15 minutes and then centrifuged at 10,000×*g* for 5 minutes to remove cellular debris. Supernatants were collected and concentrations were determined by the detergent compatible (DC) protein assay (Bio-Rad Laboratories, Hercules, CA).

In order to monitor the progress of selection, radioactive filter-binding assay was performed using a similar protocol as described previously.[2] Briefly, for aptamer ^{32}P labeling, *in vitro* transcribed RNA was purified by chromatography, then end-labeled with [γ-^{32}P] ATP using T4 polynucleotide kinase followed by G-50 column purification. Binding assays were performed by incubating ^{32}P-labeled RNA (3 pmol) with the protein at the indicated concentrations in binding buffer. The fraction of bound RNA was quantified and corrected for nonspecific background binding to nitrocellulose filters as described.[7] RNA-protein equilibrium dissociation constants[21] were determined to be equivalent to the concentration at which binding was 50% of maximal (B_{max}). A ^{32}P-labeled unselected ssRNA library was used as a negative control.

Surface plasmon resonance. Binding kinetic profiles of purified protein DHX9 (Lifeome, San Diego, CA) and aptamer S-1 were measured by SPR using a BIAcore3000 biosensor system (GE Healthcare Bio-Sciences, Piscataway, NJ). As an antigen, protein DHX9 or BSA as an protein control was immobilized on the surface of the CM5 carboxymethylated dextran matrix senor chip at pH4.5. Coupling of antigen was achieved using N-ethyl-N9-(3-dimethylaminopropyl) carbodiimide/N-hydroxysuccinimide according to the manufacturers' instructions. The running buffer was 10 mmol/l HEPES/150 mmol/l NaCl/3.4mmol/l EDTA, pH 7.4. Test samples including selected aptamer S-1, unselected library RNA, and positive control DHX9 antibody were diluted in running buffer and passed over the chip at concentrations ranging from 62.5 to 500 nmol/l. The association and dissociation rate constants (K_a and K_d) and the average affinity were determined using the nonlinear curve-fitting BIAevaluation software (BIAcore).[22]

Knockdown of DHX9 using siRNA. 119X cells (2.5×10^5 per well) were seeded in six-well plate and grown in Dulbecco's modified Eagle's medium + 10% fetal bovine serum-containing media the day before transfections. Cells were transfected twice with 100 nmol/l DHX9 siRNA (Ambion Life technologies, Grand Island, NY, siRNA ID # s4019) or control siRNA (Silencer Select negative control #1siRNA, Ambion Life technologies, catalog number: 4390843) at 24 and 48 hours using HiPerFect Transfection reagent (Qiagen) following the manufacturer's protocol. The cells were lysed 48 hours following the first transfection in RIPA (Sigma-Aldrich, St. Louis., MO) buffer containing protease inhibitor cocktail (Sigma-Aldrich). Total protein extracts (20 µg) were resolved in 4–20% sodium dodecyl sulfate-polyacrylamide gel electrophoresis gel (Bio-Rad) and transferred to polyvinylidene difluoride membrane. Western blot analysis was performed using rabbit polyclonal anti-DHX9 primary antibody (Abcam, Cambridge, MA) and horse radish peroxide-conjugated goat antirabbit secondary antibody (Invitrogen Zymed, Rockford, IL). Horse radish peroxide-conjugated anti-β-tubulin antibody (Abcam) was used as a loading control. Western blot signals were detected using enhanced chemiluminescence (ECL) reagent (Pierce ECL Western Blotting Substrate). DHX9 Western blot bands were quantitated using Image J software and were normalized to their corresponding β-tubulin (loading control) bands for calculating the reduction of DHX9 protein upon siRNA treatment (compared with the control siRNA). The cell-free lysates from DHX9 siRNA and control siRNA-treated cells were subjected to radioactive filter-binding assay using ^{32}P-radiolabeled S-1 aptamer as described previously.

RNA 3′-end labeling and RNA-protein complex pull-downs. To generate biotinylated aptamers, RNA 3′-end desthiobiotinylation kit (Pierce Biotechnology, Rockford, IL) that relies on the ability of T4 RNA ligase to attach a single desthiobiotinylated cytidine diphosphate to the 3′ end of the RNA strand was used. Briefly, 30 µl of RNA ligation mixture containing nonlabeled RNA or 50 pmol control RNA, 1 nmol biotinylated cytidine diphosphate, T4 RNA buffer 1X and ligase 40U, and PEG 30%, was incubated at 4 °C for overnight, then the RNA was recovered by extraction with chloroform:isoamyl alcohol and precipitation with 10 µl of 5 mol/l NaCl, 1µl glycogen and 300 µl ice-cold 100% ethanol.

RNA-protein complex pull-downs were performed using RNA-Protein Pull-Down kit (Pierce Biotech.). Following manufacturer's instruction, the biotinlyated RNA was first bound to the streptavidin magnetic beads. RNA-bound beads were then equilibrated in protein-RNA binding buffer before tumor protein extracts was added. The RNA-protein complex immobilized beads were incubated for 60 minutes at 4 °C followed by washing with the appropriate buffer, vortexing, and separating on a magnetic strand. Finally, the bound protein was eluted using nondenaturing biotin elution buffer. Aptamer-purified proteins

were analyzed by sodium dodecyl sulfate-polyacrylamide gel electrophoresis gel and then excised and digested *in situ* with trypsin at the Duke Proteomic Center.

RNA randomly labeling with Cy3. DuraScribe T7 Transcription kit (Epicentre) was used as previously described.[2] Briefly, PCR amplicons containing a T7 RNA polymerase promoter at the 5′ end was combined into the transcription reaction mixture, in which N6-(6-aminohexyl)-ATP (Gibco Bethesda Research Laboratories, Gaithersburg, MD) was incorporated. Following incubation at 37 °C for 6 hours, DNase I was added to remove template DNA, and the reaction mixture was then purified by chromatography and ethanol precipitation to remove unincorporated NTPs. To generate fluorescein-containing aptamers, the RNA pellets were suspended in 0.2 mol/l NaHCO3 (pH 8.2) and mixed with an equal volume of Cy3 monofunctional dye (Amersham-Pharmacia, Chicago, IL) for 1 hour at room temperature. The labeled transcripts were purified with Centricon YM-30 filters and used for below FMT imaging and tissue and cell staining.

FMT imaging. Three-dimensional *in vivo* FMT is a newly developed noninvasive imaging approach. With fluorescent probes which are in the near-infrared range, FMT is effective for imaging of tumors in a deeply embedded organ,[23] but it has not been reported for mouse models of colorectal cancer liver metastases. In our study, intrahepatic tumor-bearing mice were systemically administered Vivotag680-labeled aptamer S-1, the identified aptamer from *in vivo* selection, and MMPSense 750, a commercial fluorescent tumor marker (Perkin Elmer, Santa Clara, CA), and then subjected to FMT imaging at various times. Resulting transmission and fluorescence patterns are captured with a thermoelectrically cooled direct digital control camera, and the position and intensity of fluorescence sources are reconstructed in three dimension (TrueQuant software package, supplied with the FMT 2500). The regions of interest drawn in the upper torso encompassing the entire tumor region will be applied to all data sets and quantified in pmols. After the FMT imaging, the animals were killed and tumor mass contained liver tissues excised out for the same imaging process.

Cell fluorescent staining. 57X and 119X cells were grown to 80% confluence on chamber slides (Nalgene Nunc International, Naperville, IL) and then incubated with 0.1 µmol/l Cy3-labeled aptamer in PBS containing 2.5 µg/ml tRNA for 15 minutes at room temperature. The cells were then fixed with 4% paraformaldehyde for 20 minutes, followed by washing with PBS for three times. Fluorescent labeling of the cytoplasm was achieved using actin binding dye AlexaFluor 488 labeled phalloidin (Life Technology, Grand Island, NY), and nuclei were stained with 4,6-diamidino-2-phenylindole (Invitrogen, Eugene, Oregon). For the subcellular localization of RNA and its targeted protein, cells were permeabilized prior to triple staining with RNA, 4,6-diamidino-2-phenylindole and monoclonal antibody against DHX9 (ABcam, Cambridge, MA). Single images were taken using a Zeiss Axio Imager system cooled with a CCD camera through the Duke Light Microscopy Core Facility.

Tumor tissue fluorescent staining and immunohistochemistry. Balb/c mice bearing intrahepatic tumors growing for 12 days received an intravenous injection of Cy3-labeled aptamers (2 nmol/mouse) and a perfusion marker, Hoechst 33342 (1 mg/mouse, IV; Sigma) with 20-minute interval. At specified times, the animals were killed, and tumors were harvested and frozen at –80 °C. Frozen sections in 10-µm thickness were obtained from samples and fixed in acetone at –20 °C for 10 minutes. After blocking nonspecific protein binding with 10% normal horse serum, the slides were then incubated at 4 °C overnight in a humidified chamber with the primary antibody anti-RNA helicase A at a dilution of 1:500. After three washes in phosphate-buffered saline with Tween 20, the slides were incubated with secondary antibody AlexaFluor 488-labeled goat anti-rabbit IgG (Molecular Probes, Leiden, the Netherlands) at 1:200 at room temperature for 1 hour. After another three washes, the slides were finally mounted with Prolong Gold antifade reagent (Molecular Probes) and imaged under a fluorescent microscopy.

For tissue immunohistochemistry, after endogenous peroxidase blocking, paraffin-embedded tissue slides were incubated with primary antibody anti-RNA helicase at a dilution of 1:500 for 1 hour. After three washes with phosphate-buffered saline with Tween 20, the slides were incubated with secondary antibody biotinylated goat anti-rabbit IgG (Vector Labs, Burlingame, CA) at 1:1,000 for 1 hour and then stand in Avidin-biotin-peroxidase complex solution for 30 minutes. Sections were finally counterstained with hemtoxylin and mounted.

Western blot analysis of identified tumor protein. 57X and 119X cells and tumor tissues were homogenized in proteinase inhibitor (Roche Diagnostics, Mannheim, Gemany) containing buffer (5 mmol/l tris–HCl, pH 7.4, 2 mmol/l EDTA) followed by sonication for 15 seconds. The homogenates were then centrifuged at 4 °C for 20 minutes to remove cell debris. Supernatants were harvested and concentrations were determined by the DC protein assay (Bio-Rad Laboratories, Hercules, CA). Western blots were performed as previously described.[3] Briefly, equal amounts of protein (20 µg) were electrophoresed on a 4–20% sodium dodecyl sulfate-polyacrylamide gel electrophoresis gel and then transferred to a polyvinylidene difluoride. After blocking, the membrane was probed with primary antibodies against DHX9 overnight at 4 °C, washed three times with phosphate-buffered saline–0.05% Tween-20, followed by incubation with secondary antibody, namely, horse radish peroxide-conjugated goat antirabbit IgG (Santa Cruz, CA) for 1 hour. After washing, the signal was visualized with an ECL chemiluminescence kit (Amersham, Arlington Heights, IL). Bands were analyzed for density using Image Analysis software and normalized to loading control glyceraldehyde 3-phosphate dehydrogenase.

Acknowledgments We thank Yasheng Gao for assistance with fluorescence imaging, Greg Palmer for FMT imaging, and Scott Szafranski for SPR data. This work was supported by US national Institutes of Health grants NIH-R21-CA-128692 (B.M.C.) and Golfers Against Cancer Foundation (J.M.), and Malek Cancer Research Scientist Award (J.M.). The authors declare no conflict of interest.

1. Siegel, R, Desantis, C and Jemal, A (2014). Colorectal cancer statistics, 2014. *CA Cancer J Clin* **64**: 104–117.
2. Mi, J, Liu, Y, Rabbani, ZN, Yang, Z, Urban, JH, Sullenger, BA *et al.* (2010). *In vivo* selection of tumor-targeting RNA motifs. *Nat Chem Biol* **6**: 22–24.
3. Sarraf-Yazdi, S, Mi, J, Moeller, BJ, Niu, X, White, RR, Kontos, CD *et al.* (2008). Inhibition of *in vivo* tumor angiogenesis and growth via systemic delivery of an angiopoietin 2-specific RNA aptamer. *J Surg Res* **146**: 16–23.

4. Ray, P, Cheek, MA, Sharaf, ML, Li, N, Ellington, AD, Sullenger, BA *et al.* (2012). Aptamer-mediated delivery of chemotherapy to pancreatic cancer cells. *Nucleic Acid Ther* **22**: 295–305.
5. Ray, P, Rialon-Guevara, KL, Veras, E, Sullenger, BA and White, RR (2012). Comparing human pancreatic cell secretomes by *in vitro* aptamer selection identifies cyclophilin B as a candidate pancreatic cancer biomarker. *J Clin Invest* **122**: 1734–1741.
6. Daniels, DA, Chen, H, Hicke, BJ, Swiderek, KM and Gold, L (2003). A tenascin-C aptamer identified by tumor cell SELEX: systematic evolution of ligands by exponential enrichment. *Proc Natl Acad Sci USA* **100**: 15416–15421.
7. Liu, Y, Kuan, CT, Mi, J, Zhang, X, Clary, BM, Bigner, DD *et al.* (2009). Aptamers selected against the unglycosylated EGFRvIII ectodomain and delivered intracellularly reduce membrane-bound EGFRvIII and induce apoptosis. *Biol Chem* **390**: 137–144.
8. White, R, Rusconi, C, Scardino, E, Wolberg, A, Lawson, J, Hoffman, M *et al.* (2001). Generation of species cross-reactive aptamers using "toggle" SELEX. *Mol Ther* **4**: 567–573.
9. Liu, M, Roth, A, Yu, M, Morris, R, Bersani, F, Rivera, MN *et al.* (2013). The IGF2 intronic miR-483 selectively enhances transcription from IGF2 fetal promoters and enhances tumorigenesis. *Genes Dev* **27**: 2543–2548.
10. Lai, YH, Cheng, J, Cheng, D, Feasel, ME, Beste, KD, Peng, J *et al.* (2011). SOX4 interacts with plakoglobin in a Wnt3a-dependent manner in prostate cancer cells. *BMC Cell Biol* **12**: 50.
11. Zhong, X and Safa, AR (2004). RNA helicase A in the MEF1 transcription factor complex up-regulates the MDR1 gene in multidrug-resistant cancer cells. *J Biol Chem* **279**: 17134–17141.
12. Lee, T, Di Paola, D, Malina, A, Mills, JR, Kreps, A, Grosse, F *et al.* (2014). Suppression of the DHX9 helicase induces premature senescence in human diploid fibroblasts in a p53-dependent manner. *J Biol Chem* **289**: 22798–22814.
13. Fuller-Pace, FV (2006). DExD/H box RNA helicases: multifunctional proteins with important roles in transcriptional regulation. *Nucleic Acids Res* **34**: 4206–4215.
14. Jain, A, Bacolla, A, Chakraborty, P, Grosse, F and Vasquez, KM (2010). Human DHX9 helicase unwinds triple-helical DNA structures. *Biochemistry* **49**: 6992–6999.
15. Bläss, S, Meier, C, Vohr, HW, Schwochau, M, Specker, C and Burmester, GR (1998). The p68 autoantigen characteristic of rheumatoid arthritis is reactive with carbohydrate epitope specific autoantibodies. *Ann Rheum Dis* **57**: 220–225.
16. Srivastava, M and Pollard, HB (1999). Molecular dissection of nucleolin's role in growth and cell proliferation: new insights. *FASEB J* **13**: 1911–1922.
17. Banroques, J and Tanner, NK (2015). Bioinformatics and biochemical methods to study the structural and functional elements of DEAD-box RNA helicases. *Methods Mol Biol* **1259**: 165–181.
18. Abdelhaleem, M (2004). Do human RNA helicases have a role in cancer? *Biochim Biophys Acta* **1704**: 37–46.
19. Guénard, F, Labrie, Y, Ouellette, G, Beauparlant, CJ and Durocher, F; INHERIT BRCAs (2009). Genetic sequence variations of BRCA1-interacting genes AURKA, BAP1, BARD1 and DHX9 in French Canadian families with high risk of breast cancer. *J Hum Genet* **54**: 152–161.
20. Wei, X, Pacyna-Gengelbach, M, Schlüns, K, An, Q, Gao, Y, Cheng, S *et al.* (2004). Analysis of the RNA helicase A gene in human lung cancer. *Oncol Rep* **11**: 253–258.
21. Thiel, WH, Bair, T, Peek, AS, Liu, X, Dassie, J, Stockdale, KR *et al.* (2012). Rapid identification of cell-specific, internalizing RNA aptamers with bioinformatics analyses of a cell-based aptamer selection. *PLoS One* **7**: e43836.
22. Kuan, CT, Wakiya, K, Keir, ST, Li, J, Herndon, JE 2nd, Pastan, I *et al.* (2011). Affinity-matured anti-glycoprotein NMB recombinant immunotoxins targeting malignant gliomas and melanomas. *Int J Cancer* **129**: 111–121.
23. Bao, B, Groves, K, Zhang, J, Handy, E, Kennedy, P, Cuneo, G. *et al.* (2012) *In vivo* imaging and quantification of carbonic anhydrase IX expression as an endogenous biomarker of tumor hypoxia. *PLoS One* **7**: e50860. doi: 10.1371/journal.pone.0050860.

This work is licensed under a Creative Commons Attribution-NonCommercial-ShareAlike 4.0 International License. The images or other third party material in this article are included in the article's Creative Commons license, unless indicated otherwise in the credit line; if the material is not included under the Creative Commons license, users will need to obtain permission from the license holder to reproduce the material. To view a copy of this license, visit http://creativecommons.org/licenses/by-nc-sa/4.0/

© Jing Mi *et al.* (2016)